Multiphasic Desensitization of the $GABA_A$ Receptor in Outside-Out Patches

James J. Celentano and Robert K. S. Wong
Deptartment of Pharmacology, State University of New York Health Science Center, Brooklyn, New York 11203 USA

ABSTRACT $GABA_A$ receptor function was studied in outside-out patches from guinea pig hippocampal neurons using a drug application system with an exchange time of under 1.5 ms. Application of GABA to these patches induced a Cl^- conductance that desensitized with prolonged exposure. Increasing GABA concentrations induced larger conductance increases that were associated with more complex patterns of desensitization. Smaller GABA responses desensitized with monophasic kinetics, whereas larger responses displayed bi- and triphasic kinetics. Desensitization of the response to 1 mM GABA was triphasic in about 70% of the patches (τ = 15.4, 207, and 1370 ms) and biphasic in about 30% of the patches (τ = 44 and 725 ms). All phases of desensitization reversed at the Cl^- equilibrium potential. Over the concentration range from 3 μM to 3 mM, both the rate and the extent of desensitization increased; however, complete desensitization was rarely observed. The increase in desensitization rate was due to an increase in the relative contribution of the faster phases with increasing GABA. The time constants of the three phases were independent of concentration. The different phases are not mediated by separate receptor populations, because double pulse experiments demonstrated interconversion among the fastest phase and the two slower phases. We demonstrate the plausibility of a model in which multiphasic desensitization is a consequence of the faster association rate at higher GABA concentrations.

The $GABA_A$ receptor is a ligand-gated chloride ion channel found on the surface of virtually all vertebrate central neurons (Krnjevic, 1974; Sivilotti and Nistri, 1991). It is of interest as an inhibitory neurotransmitter receptor, as the site of action of many toxic and therapeutic agents, and as a model system for the study of allosteric interactions. Of particular importance is the presence of at least five distinct binding sites (benzodiazepine, barbiturate, steroid, picrotoxin, and divalent cation) through which a wide variety of agents exert allosteric control over channel function (Olsen, 1982; Trifiletti et al., 1985; Haefely and Polc, 1986; Kirkness and Turner, 1988; Holland et al., 1990; Celentano et al., 1991; Sivilotti and Nistri, 1991). During prolonged exposure to high concentrations of agonist, the receptor undergoes reversible desensitization (Ben-Ari et al., 1979; Numann and Wong, 1984; Thalmann and Hershkowitz, 1985; Akaike et al., 1986; Mierlak and Farb, 1988; Frosch et al., 1992; Oh and Dichter, 1992). Although the physiological significance of desensitization remains unclear, this phenomenon is observed in many ligand-gated ion channels (Dudel et al., 1992). The mechanisms that underlie desensitization are important to the understanding of receptor function and, ultimately, to the understanding of receptor modulation.

The rate at which $GABA_A$ receptor desensitization occurs varies greatly among different preparations. Electrophysiological studies on neurons from a variety of sources reveal desensitization time constants ranging from hundreds of milliseconds to tens of seconds (Ben-Ari et al., 1979; Numann and Wong, 1984; Thalmann and Hershkowitz, 1985; Akaike et al., 1986; Mierlak and Farb, 1988; Frosch et al., 1992; Oh and Dichter, 1992). Because GABA was applied relatively slowly (tens to hundreds of milliseconds), faster rates of desensitization cannot be ruled out. The quench-flow technique, by which neuronal membrane vesicles were exposed to agonist in under 5 ms, revealed biphasic desensitization ($t_{1/2}$ = 32 and 533 ms) of GABA-induced $^{36}Cl^-$ flux (Cash and Subbarao, 1987). Although electrophysiological studies using rapid drug application techniques have demonstrated desensitization on the millisecond time scale for the acetylcholine (Franke et al., 1991; Dilger and Liu, 1992) and glutamate receptors (Trussell and Fischbach, 1989; Sather et al., 1990), similar studies have not been conducted for the vertebrate $GABA_A$ receptor (Newland et al., 1991).

In this study, we developed a seven-barrel flow tube method by which the solution around the tip of a patch electrode can be exchanged in under 1.5 ms. The rapid application of high concentrations of GABA reveals multiphasic desensitization with rates comparable to those observed in membrane vesicles. The different phases of desensitization are not mediated by separate receptor populations, but by a single population with at least three desensitized states. The data obtained in this study can be qualitatively reproduced by a simple model in which the rate of GABA association plays a critical role in the observation of receptor desensitization. At low concentrations association is slow, and desensitization is concurrent with activation. At high concentrations association is fast, and activation precedes desensitization, resulting in a larger response with additional transient components.

METHODS

Isolation of hippocampal neurons

Pyramidal cells were acutely isolated from the CA1 field of the guinea pig hippocampus by the method of Kay and Wong (1986). Briefly, animals

Received for publication 24 September 1993 and in final form 14 January 1994.

Address reprint requests to James J. Celentano, Department of Pharmacology, Box 29, SUNY HSC at Brooklyn, 450 Clarkson Avenue, Brooklyn, NY 11203. Tel.: 718-270-3941; Fax: 718-270-2241.

0006-3495/94/04/1039/12 $2.00

(250–300 g) were anesthetized with ketamine (40 mg, i.p.) and sacrificed by decapitation. The brain was quickly removed and cooled in ice cold PIPES saline (in mM: 120 NaCl, 5 KCl, 1 $CaCl_2$, 1 $MgCl_2$, 25 D-glucose, 20 PIPES; pH 7.0 with NaOH). The hippocampus was dissected from the rest of the brain and cut into 650-μm slices on a McIlwain tissue chopper.

The CA1 pyramidal cell layer was dissected out and cut into fragments of about 1 mm^2. The fragments were treated with trypsin (Type XI, Sigma Chemical Co., St. Louis, MO) at 0.6–0.8 mg/ml in PIPES saline at 32°C under a continuous flow of 95% O_2 for 90 min, after which time the trypsin solution was replaced with PIPES saline and maintained at room temperature for at least 1 h before use.

One or two fragments were transferred to a 35 mm polylysine-coated culture dish containing DMEM (Dulbecco's modified Eagle's medium with 25 mM HEPES and 25 mM D-glucose, pH 7.4). Fragments were triturated with fire-polished Pasteur pipettes (0.5 and 0.2 mm i.d. at the tip). Neurons were allowed to settle to the bottom of the dish (10 min), and DMEM was replaced with standard recording buffer (in mM: 145 NaCl, 1 $MgCl_2$, 1 $CaCl_2$, 10 HEPES, 25 D-glucose; pH 7.4 with NaOH).

Electrophysiology

Recordings were done on the stage of an inverted phase contrast microscope enclosed in a Faraday cage. Pyramidal cells, identified morphologically, made up the vast majority of the isolated neurons. Patch electrodes (8–13 MΩ) were pulled on a PP-83 microelectrode puller (Narishige, Tokyo, Japan) from thin-walled borosilicate glass (World Precision Instruments, New Haven, CT) and used without fire polishing. Unless otherwise indicated, electrodes were filled with standard electrode buffer (in mM: 130 Tris HCl/Trizma base, 10 HEPES, 4 $MgCl_2$, 3 NaCl, 4 Na_2ATP, 10 EGTA; pH 7.3 with methanesulfonic acid, final Cl^- concentration 11 or 46 mM). Outside-out patches obtained using standard techniques (Hamill et al., 1981) typically had resistances of 1 to 5 gigaohms.

Voltage-clamp currents were recorded using a List EP-7 patch-clamp amplifier (List Electronic, Darmstadt, FRG). Current traces were low pass-filtered (4 kHz) using an 8-pole Bessel filter (Frequency Devices, Haverhill, MA), digitized (400 Hz, unless otherwise stated) using an on-line data acquisition system (Lab Master, Scientific Solutions, Solon, OH), and stored on disk (pClamp, Axon instruments, Foster City, CA) for further analysis off-line.

Drug application

We have developed a modified version of the seven-barrel puffer system (Chan et al., 1983) in which drug solution is expelled by gravity flow (45 cm of H_2O) from a seven-barrel flow tube with large (200 μm) tip openings. Seven-barrel glass (Frederick Haer & Co., Brunswick, ME) was pulled to a sharp tip on a Narishige PE-2 microelectrode puller. Each of the six outer barrels was scored with a diamond-tipped pen at the point where the total diameter was 1 mm, which corresponds to an internal diameter of 0.2 mm for each of the seven barrels. The tip was broken off, and only those with a flush break in which all seven barrels were of equal length were used.

Flow through the barrels was controlled by seven miniature inert valves (HPV, Hamilton Co., Reno, NV). In earlier experiments, each flow tube barrel was connected to its controlling valve by a 22-g needle and a standard anesthesia extension set (i.d. 3.5 mm). In later experiments, this connection was made by a standard infusion set with a 23-g needle and a smaller diameter tubing (i.d. 1.2 mm). The decrease in tubing diameter substantially improved the performance of the flow tube, probably by decreasing the compliance of the connection between the flow-tube and the valves.

Each of the seven controlling valves was connected by way of a simple mechanical linkage to an air cylinder with a 0.5" stroke (3PS-1/2, Clippard Instrument Laboratory, Cincinnati, OH). During wash periods, the center barrel was open, and the six outer barrels were closed. Solution exchange was initiated by a Picospritzer (General Valve Corp., Fairfield, NJ), which simultaneously pressurized the cylinders controlling the center barrel and one of the six outer barrels. The valves were arranged so that the effect was to close the center barrel and open the designated outer barrel. To maximize the solution exchange rate, the flow rate of the center barrel (0.6 ml/min) was set slower than that of the outer barrels (2 ml/min). This was necessary because the mechanical delay (~200 ms) associated with pressurizing the cylinders is slightly longer for the center valve than the outer valves. This difference was not observed when switching among the six outer barrels while the center barrel remained closed. The identical procedure was used for both drug application, in which the center barrel contained wash solution while the outer barrels contained drug solution, and for testing the speed of solution exchange, in which the center barrel contained the preexchange solution while the outer barrels contained postexchange solutions.

The flow tube was positioned 0.3 mm above the surface of the dish at an angle of 45° and a distance of 1.5 mm from the recording electrode (Fig. 1 *A*). Under direct visualization, dye solutions exit each barrel in a well delineated column and spread out over the bottom of the dish forming a plume about 2 mm wide at the point of the electrode. Because the plume is of limited thickness, the electrode must be within 40 μm of the bottom of the dish to ensure rapid and complete exchange. Despite small differences in the relative position of each barrel, all seven barrels were capable of rapid exchange without repositioning of the flow tube or the electrode.

As flow from the center barrel is discontinued, flow from one of the six outer barrels is initiated, and the interface between the two solutions sweeps across the tip of the electrode. To ensure rapid exchange, it is necessary to avoid turbulent flow that increases mixing at the interface. Water flowing at a rate of 100 cm/s through an inner diameter of 0.2 mm has a Reynolds number of 200, which is well below the critical value of 2000, above which flow becomes turbulent (Kreider, 1985). At a flow rate of 100 cm/s along the surface of the dish, the critical length at which turbulence begins to develop is 50 cm (Kreider, 1985). In these experiments, the distance traveled by the expelled solution along the bottom of the dish was no more than 1.5 mm.

GABA response

The center barrel of the drug delivery system was filled with standard recording buffer, and the six outer barrels were filled with various concentrations of GABA in standard recording buffer. At 0 mV holding potential, application of GABA induced an outward current. Unless otherwise stated, the duration of GABA application was 3 s. Successive GABA applications were separated by 1–2 min recovery periods, during which the patch was washed by a continuous stream of standard recording buffer from the center barrel.

Data analysis

Curve-fitting was done using software written by Dr. Terrell T. Gibbs, which combines patternsearch (Hooke and Jeeves, 1961; Colquhoun, 1971) and simplex (Nedler and Mead, 1965; Motulsky and Ransnas, 1987) algorithms. These algorithms maximize the goodness-of-fit by manipulating parameters so as to minimize the residual sum of squares. All curve-fitting results were inspected visually by plotting the theoretical and observed data together. Accurate results were obtained consistently when fitting idealized data to which random noise (comparable to experimental noise) was added.

The decay phase of the GABA response was fit to a single, double or triple exponential equation

$$I(t) = I_{ss} + I_f e^{(-t/\tau_f)} + I_i e^{(-t/\tau_i)} + I_s e^{(-t/\tau_s)}$$

where I_{ss} represents the steady-state current at equilibrium, I_f, I_i, and I_s represent the magnitude of the current that desensitizes with fast, intermediate, and slow kinetics, respectively, and τ_f, τ_i, and τ_s are the time constants of the fast, intermediate, and slow phases of desensitization, respectively. The time at which the rising phase is approximately half maximum is defined as $t = 0$. The F-test (5% confidence limit) was applied to the residual sum of squares to determine the appropriateness of using an additional component to describe the desensitization phase (Munson and Rodbard, 1980; Zar, 1984; Motulsky and Ransnas, 1987).

To accommodate a limit on the number of data points and to speed up the fitting process, the effective sampling interval was extended from 2.5 to 5 ms (by replacing each pair of points with their average) for the range of 100–200 ms after the start of the GABA response. For curve-fitting

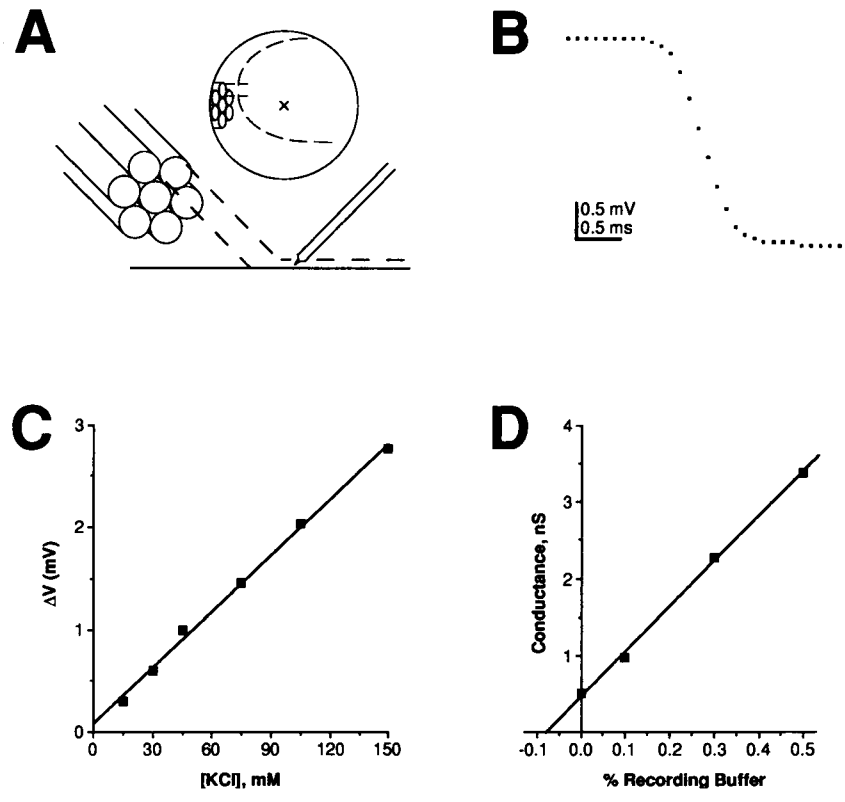

FIGURE 1 Calibration of the seven-barrel flow tube. (*A*) Barrel #1 of the seven-barrel flow tube is shown coating the dish surface with drug solution. Barrels are numbered clockwise (#1-#6, center is #7). Inset shows the plume of expelled solution (barrel #2) viewed from above. The cross indicates the position of the electrode. (*B*) The junction potential of an open electrode (filled with 1 M KCl) during a step from NaCl to KCl (150 mM). The exchange time (10–90%) is approximately 600 μs. The sampling rate was 10 kHz. (*C*) The magnitude of the junction potential shift, as in *B*, during a series of steps from 150 mM NaCl to a mixture of NaCl and KCl (150 mM total) is plotted against the concentration of KCl. Over this range, the shift is directly proportional to the concentration of KCl. (*D*) The conductance of an open electrode (filled with standard electrode buffer) was measured after replacement of the external solution (standard recording buffer) with either 91 mM glucose (0%) or a mixture of recording buffer (0.1–0.5%, v/v) and 91 mM glucose. The conductance is plotted against the percentage of recording buffer in the expelled solution. Back extrapolation to 0 nS indicates that expelled solution is diluted by no more than 0.1% with bulk solution. The electrode conductance was 244 nS in standard recording buffer before application of 91 mM glucose.

purposes these points were assigned weights of 2. Similarly, the interval for all points later than 200 ms was extended to 10 ms, and each point assigned a weight of 4. This procedure did not effect curve-fitting results using idealized data.

To determine the characteristics of the GABA concentration-response relationship, pooled data were weighted by error and fit to the logistic equation (De Lean et al., 1978)

$$\text{Response} = \frac{\text{Response}_{MAX} \times [\text{GABA}]^n}{\text{EC}_{50}^n + [\text{GABA}]^n}$$

where Response_{MAX} is the maximum GABA response, EC_{50} is the concentration of GABA inducing 50% of the maximum response, and n is the Hill coefficient. Dose-response curves were generated for the peak current (I_p), which is the sum of I_{ss}, I_f, I_i, and I_s, as well as for the magnitude of the current without the fast phase ($I_i + I_s + I_{ss}$), and for the magnitude of the current without the fast and intermediate phases ($I_s + I_{ss}$).

Student's *t*-test was used for making comparisons between two groups, and ANOVA was used for making comparisons among three or more groups. Significance was defined as $p < 0.05$.

GABA$_A$ receptor modeling

The results from this paper were used to generate a kinetic model of activation and desensitization. The equilibrium constants for each reaction were first determined from steady-state values (EC_{50} and extent of desensitization), and the absolute kinetic constants were determined using the measured time constants (rise and desensitization). Simulations were carried out using a Runge-Kutta-4 with at constant Δt of 0.1 ms. No significant changes occurred when a Δt of 0.05 was tested.

RESULTS

Test of drug application system

Three methods were employed to test the reliability of the seven-barrel flow tube. The speed of solution exchange was tested by monitoring the junction potential of a patch electrode (filled with 1 M KCl) during an exchange of 150 mM NaCl with 150 mM KCl in the outside solution. Because of the difference in mobility between sodium and potassium, this exchange results in a negative shift in the junction potential (Fig. 1 *B*). The exchange time is the time required for a 10–90% shift in junction potential. Each flow tube was tested in this manner before use. Only those in which all six outer barrels had exchange times of 1.5 ms or less were used.

Variability among the exchange times of the six outer barrels is due to differences in flow characteristics rather than the relative position of the individual barrels. Exchange times were not significantly affected when the relative positions are altered by rotating the flow tube, however, when the inner diameter of the tubing used to connect the barrels to their respective valves was decreased from 3.5 to 1.2 mm, the exchange times decreased from a range of 0.4–1.5 ms to a range of 0.2–0.8 ms. Data presented in this report are from experiments using both configurations.

The junction potential shift method assumes that the magnitude of the shift is linearly related to the concentration of KCl around the tip of the electrode. We tested this assumption by applying mixtures of NaCl and KCl to an open electrode (Fig. 1 *C*). The magnitude of the shift does not saturate over the concentration range studied, but increases linearly with the amount of KCl applied.

To test for mixing between expelled and bulk solutions, the conductance of an electrode filled with standard electrode buffer was monitored after the replacement of standard recording buffer with solutions of lower ionic strength. When recording buffer was replaced with 91 mM glucose (no added

ions), electrode conductance decreased by a factor of several hundred. To simulate mixing, flow tube barrels were filled with solutions containing 91 mM glucose to which small amounts of recording buffer were added. The addition of 0.5% (v/v) recording buffer increased electrode conductance by more than a factor of 6 (Fig. 1 *D*). When the plot of conductance versus percentage of recording buffer is extrapolated back to 0 nS, the intercept predicts less than 0.1% dilution of the expelled solution with bulk solution.

The effect of a membrane patch on the speed of exchange was also tested. Electrodes were filled with standard electrode buffer without Na_2ATP in which Tris was replaced with 130 mM KCl, and the pH was adjusted to 7.3 with KOH. The exchange time was measured by monitoring current through outside-out patches in voltage-clamp mode during an increase in extracellular K^+ from 5 to 140 mM. At a holding potential of 0 mV, this change resulted in a rapid reduction of the resting membrane current as the K^+ concentration gradient was eliminated. In a series of four patches, the exchange time was 0.49 ± 0.14 ms. Each patch was disrupted, and the exchange time of the open electrode was tested by monitoring the current at 0 mV during the same solution exchange. The exchange time for the same four electrodes was 0.40 ± 0.06 ms. The presence of a membrane patch at the tip of the electrode does not significantly affect the rate of solution exchange.

GABA receptor desensitization

Using a single seven-barrel flow tube, we studied the rise time of the membrane conductance increase induced by 1 mM GABA expelled from each of the six outer barrels (Table 1). The variability in exchange times (measured using the junction potential shift method) among the six outer barrels did not significantly affect the peak response or the initial rate of desensitization. The rise times of the GABA responses were only slightly longer (0.20 ± 0.09 ms) than the exchange times for the same six barrels.

Fig. 2 *A* shows representative traces of six concentrations of GABA applied to a single patch. We estimate an average of about 230 receptors/patch (based on 23 pS per channel (Gray and Johnston, 1985) and an 81% probability of opening (Newland et al., 1991) during the peak response to 1 mM GABA). The number of receptors/patch ranges from as few

TABLE 1 Comparison of flow-tube barrels

Barrel	Exchange time (KCl)	Rise time (GABA)	Relative maximum	τ
#1	0.49 ± 0.05	1.03 ± 0.32	1.020 ± 0.097	9.7 ± 1.8
#2	0.32 ± 0.04	0.50 ± 0.09	1.033 ± 0.106	8.4 ± 2.5
#3	0.51 ± 0.09	0.70 ± 0.12	1.000	10.8 ± 2.4
#4	0.78 ± 0.08	1.06 ± 0.25	0.992 ± 0.029	10.8 ± 2.9
#5	1.16 ± 0.11	1.00 ± 0.10	0.977 ± 0.031	9.9 ± 3.5
#6	0.80 ± 0.27	0.95 ± 0.33	1.003 ± 0.100	9.1 ± 2.0

The solution exchange time (in ms) was tested using the junction potential shift for a series of five open electrodes (KCl). The average exchange time for the six barrels was 0.676 ± 0.12. The same seven-barrel flow tube was used to apply 1 mM GABA to a series of outside out patches. The rise time of the GABA response (GABA) was measured for each barrel (n = 3–4). The average rise time for the six barrels was 0.873 ± 0.091 ms. The maximum response for each barrel was scaled to the maximum response to barrel #3. The first 45 ms of the desensitization phase was fit to a single exponential, and the time constant (τ) expressed in ms. Despite small differences in the rise times among the six barrels, there was no significant difference among the maxima, or the desensitization time constants. The connection between the barrels and the valves was made with large (3.5 mm i.d.) tubing. The sampling rate was 10 kHz. All values are ± SE.

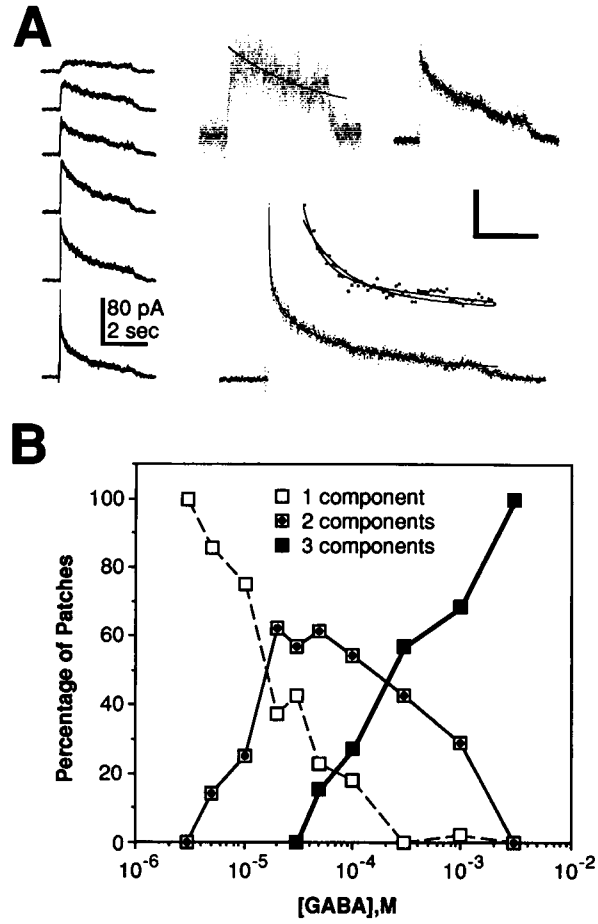

FIGURE 2 Increasing GABA concentration increases the complexity of desensitization kinetics. (*A*) Response to increasing concentrations of GABA in a single patch are shown at the same scale (*left*). Concentrations are (from top) 3, 10, 20, 50, 100, and 1000 μM. Desensitization is best fit by a single exponential in the top two traces, by a double exponential in the middle two traces, and by a triple exponential in the bottom two traces. Selected traces are reproduced at different scales with curve-fitting results, top center: 3 μM GABA, 10 pA, 2 s; top right: 20 μM GABA, 30 pA, 2 s; bottom right: 1000 μM GABA, 40 pA, 1 s and 50 ms. Initial response to 1 mM GABA is shown with results of both two and three component fits. Addition of the third component significantly improves the quality of the fit ($F = 44.76, p < 0.01$). Intracellular Cl^-: 46 mM, holding potential: 0 mV. (*B*) A series of GABA concentrations were applied to at least seven patches, and the desensitization was characterized according to the number of exponential components giving the best fit. The percentage of patches best fit by one (open symbols), two (dotted symbols), or three (filled symbols) components is plotted against GABA concentration. The likelihood of observing multiple phases of desensitization increases with increasing GABA concentration. Where possible throughout this report, open symbols are associated with the slow component, dotted symbols with the intermediate component, and filled symbols with the fast component.

as 50 to as many as 800. Individual channel events were not observed in this study. GABA responses were studied from 3 to 30 min after the establishment of the outside-out patch configuration. During this time, little or no run-down (Gyenes et al., 1988; Stelzer et al., 1988; Chen et al., 1990) was observed.

As higher concentrations of GABA were applied, there was an increase in both the peak response and the number of components required to fit the desensitization. The F-test was applied to the residual sum of squares to determine the number of components required to give the best fit (Fig. 2 *A*). Only when the fit was significantly improved ($p < 0.05$) was a larger number of components required. In many cases, fitting to an exponential equation with unnecessary components yielded more than one component with the same time constant, and no improvement in the residual sum of squares.

As the GABA concentration increased, desensitization changed from predominantly a single exponential to a double and then to a triple exponential (Fig. 2 *B*). The transition was not abrupt, and more than one pattern was observed for all but the highest and lowest concentrations studied. The response to 1 mM GABA was most extensively studied. When only those patches with intracellular Cl^- of 46 mM were considered, the maximum response at a holding potential of 0 mV was significantly lower in the patches showing biphasic kinetics (62.7 ± 16.7 pA, $n = 9$), than those showing triphasic kinetics (158 ± 27 pA, $n = 26$).

The effect of agonist concentration on desensitization is typically studied by measuring the extent and the rate of desensitization. In this study, the existence of multiple phases of desensitization complicates this analysis. The overall extent of desensitization (due to all three phases) increased with GABA concentration (Fig. 3 *A*, open symbols). The intermediate and fast phases had different thresholds, but also increased with GABA concentration. Because of a greater relative contribution of the faster phases, the overall rate of desensitization increased with increasing GABA; however, the three phases each had inherent time constants that were independent of concentration (Fig. 3 *B*). The principle effect of increasing GABA is to increase the extent and complexity of desensitization without substantially influencing the rate of the individual phases.

The average τ of the rapid phase of desensitization was 15.4 ± 2.6 ms ($n = 28$) for the response to 1 mM GABA. This determination was probably not adversely affected by the sampling rate of 400 Hz, which yields an average of 6 points/time constant. Curve-fitting idealized data (triple exponential decay, 2.5 ms per point, time constants of 15, 200, and 1000 ms) yielded accurate values both with and without the addition of random noise to the data. Averaging the later points, as described in Methods, also had no effect on curve-fitting results. In addition, a comparable value for τ_f (10.0 ± 2.5 ms, $n = 4$) was obtained when the initial phase of the response to 1 mM GABA was examined at a sampling rate of 10 kHz (Table 1).

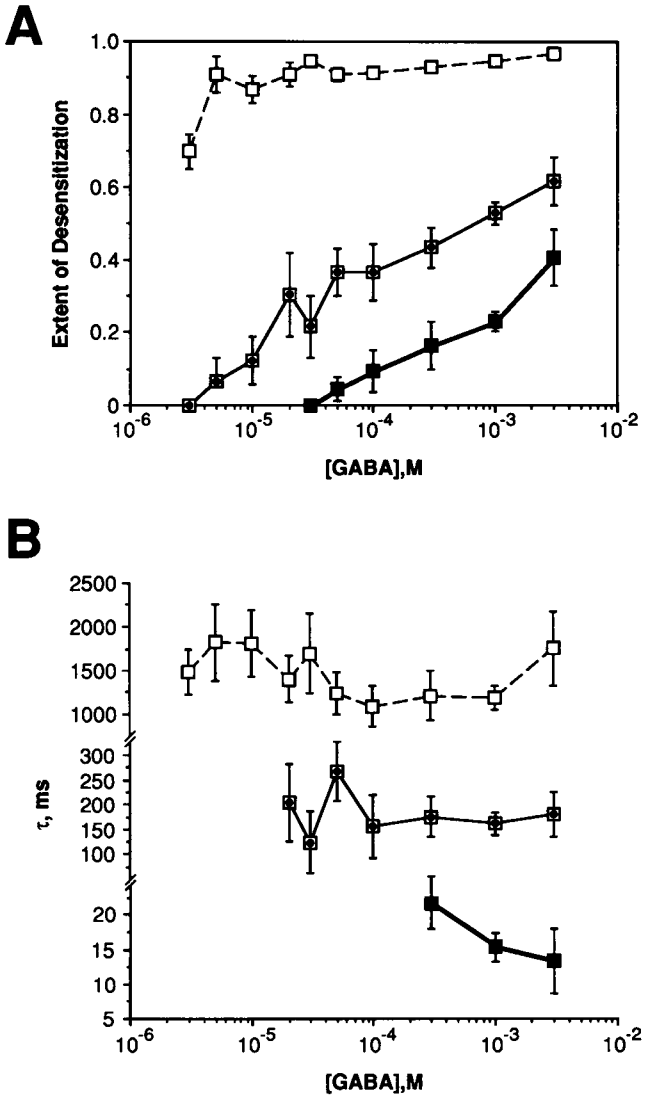

FIGURE 3 Effects of GABA concentration on desensitization parameters. (*A*) The fraction of the peak response desensitized by GABA (extent of desensitization) is plotted against GABA concentration. The extent of total desensitization (open symbols), is given by $(I_f + I_i + I_s)/I_p$. The extent of the fast plus intermediate phases (dotted symbols) is given by $(I_i + I_s)/I_p$, and the extent of the fast phase alone (filled symbols) is given by I_f/I_p. GABA concentration has a substantial effect on the extent of desensitization. Each point represents the average of ≥7 patches ± SE. (*B*) The rate of desensitization expressed as a time constant (τ) is plotted against GABA concentration. The slow (open symbols), intermediate (dotted symbols), and fast (filled symbols) time constants are unchanged over the concentration range observed. For all three phases, there is no significant difference among the points. Each point represents the average of ≥4 patches ± SE.

GABA$_A$ dose-response relationship

In addition to having inherent time constants, each phase of GABA$_A$ receptor desensitization has an inherent magnitude. To describe the dose-response curves, the fast and intermediate components will refer to the magnitude of the fast and intermediate phases of desensitization, respectively, whereas the slow component will refer to the sum of both the slow phase and the steady state current ($I_s + I_{ss}$). As the GABA

concentration increases from 50 to 1000 μM, the fast component develops without an increase in the intermediate or slow components (Fig. 4 *A*). Data from many patches were scaled to the peak response to 1 mM GABA pooled and plotted against concentration, giving the dose-response curve shown in Fig. 4 *B*. The peak response had an EC_{50} of 25.7 μM, a Hill coefficient of 0.91, and a maximum of 1.04. When the slow component alone and the slow plus intermediate components were scaled to the peak response to 1 mM GABA, they reached distinct maxima (0.49 and 0.78, respectively) with lower EC_{50} values (7.8 and 14.5 μM, respectively) and comparable Hill coefficients (1.03 and 1.07, respectively).

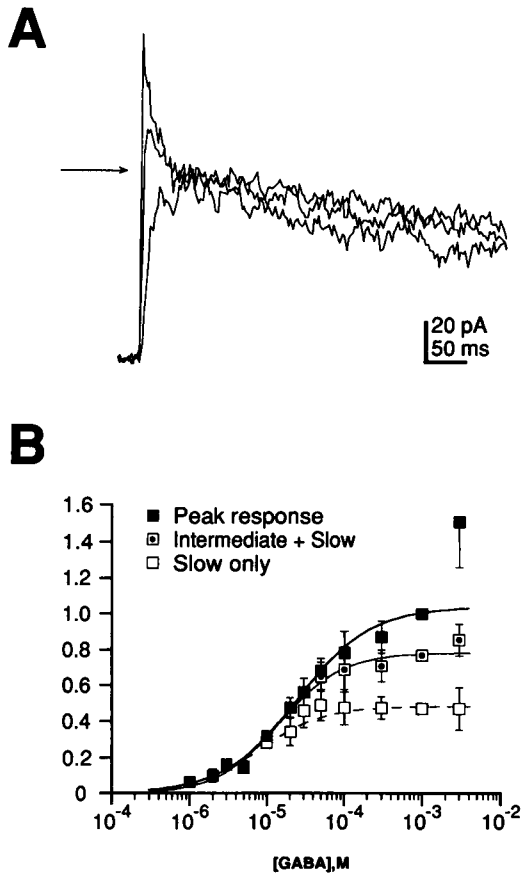

FIGURE 4 GABA dose-response relationship. (*A*) Superimposed traces from a single patch show the initial response to 50, 100, and 1000 μM GABA. The response to 50 μM GABA had a peak of 91 pA (*arrow*) and showed biphasic kinetics of desensitization. The additional current induced by 100 and 1000 μM GABA desensitized with rapid kinetics. The increase in the peak associated with 100 and 1000 μM GABA is due, therefore, exclusively to the development of a new (third) component of the GABA-induced current that desensitizes with rapid kinetics. The magnitudes of the intermediate plus slow components ($I_i + I_s + I_{ss}$) of the responses to 100 and 1000 μM GABA (86 and 96 pA, respectively) are similar to the peak response to 50 μM GABA. Intracellular Cl^-: 46 mM, holding potential: 0 mV. (*B*) Data from individual patches were scaled to the peak response to 1 mM GABA and plotted against GABA concentration. The peak response (filled symbols) has a maximum of 1.04, an EC_{50} of 25.7 μM, and a Hill coefficient of 0.91. When the fast component is excluded, the sum of the intermediate and slow components (dotted symbols) has a maximum of 0.784, an EC_{50} of 14.5 μM, and a Hill coefficient of 1.07. The slow component ($I_s + I_{ss}$, open symbols) has a maximum of 0.485, an EC_{50} of 7.82 μM, and a Hill coefficient of 1.03. Each point represents the average of ≥6 patches ± SE. Smooth curves are drawn from the logistic equation.

Are the different phases of $GABA_A$ receptor desensitization mediated by separate receptor populations?

It has been suggested that the fast and slow phases of $GABA_A$ receptor desensitization are mediated by distinct receptor populations (Cash and Subbarao, 1987). The results described above can be explained by the presence of three receptor populations with differing agonist affinities and rates of desensitization. To test for differences in ion selectivity we measured the response to 1 mM GABA in six patches at 0, −20, and −40 mV. A single reversal potential (at the Cl^- equilibrium potential) was observed for all phases of desensitization (Fig. 5). The time constant of the fast phase (seen in 5 of 6 patches) was voltage-independent (τ_f = 15 ± 2, 25 ± 12, 15 ± 4, for 0, −20, and −40 mV, respectively).

The development of the fast phase at GABA concentrations above 50 μM suggests the presence of a low affinity site. If the fast phase is mediated by a distinct population of low affinity receptors, only a small fraction of these will be occupied in the presence of 30 μM GABA. We found, however, that a prepulse of 30 μM GABA completely eliminates the fast phase of the response to 1 mM GABA (Fig. 6). These results demonstrate that binding sites on receptors mediating the fast phase are not exclusively low affinity. These receptors must have at least one high affinity binding site at which 30 μM GABA acts to blunt the fast phase. Given that glutamate channels can desensitize without opening (Trussell

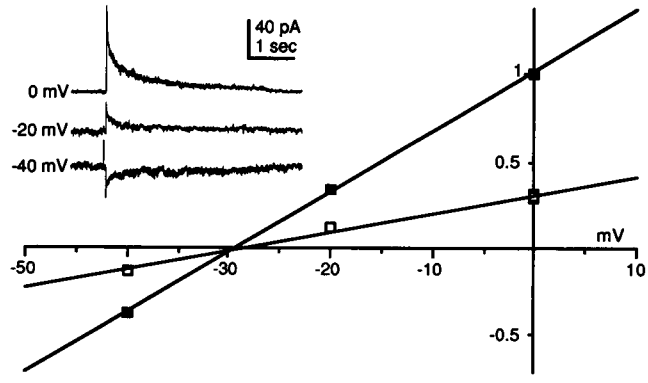

FIGURE 5 The GABA response reverses at the Cl^- equilibrium potential. Response to 1 mM GABA was measured at holding potentials of 0, −20, and −40 mV. Results were fit to double or triple exponentials and scaled to the peak response at 0 mV. Intracellular Cl^- was 46 mM, giving a Cl^- equilibrium potential of −29.7 mV. The reversal potential for the peak response (filled symbols) was −29.4 mV. The magnitude of the fast phase (observed in 5 out 6 patches) was also scaled to the peak response at 0 mV (open symbol) and had a reversal potential of −28.8 mV. Each point represents the average ± SE. Points without error bars have SE smaller than the size of the symbol. Inset shows representative traces from a single patch.

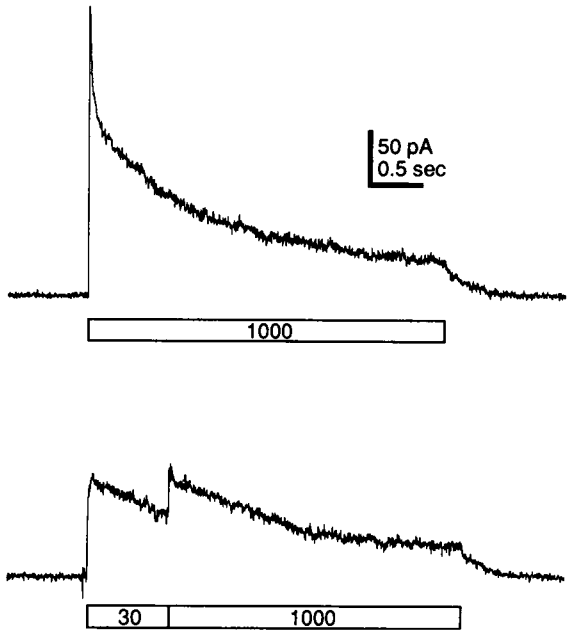

FIGURE 6 A 30 μM prepulse of GABA blunts the rapidly desensitizing response to 1 mM GABA. The fast phase of the response to 1 mM GABA (*top*) was not observed when application followed a prepulse of 30 μM GABA (*bottom*). Consecutive traces from a single patch. Holding potential: 0 mV, intracellular Cl^-: 46 mM. Similar results were obtained in four other patches.

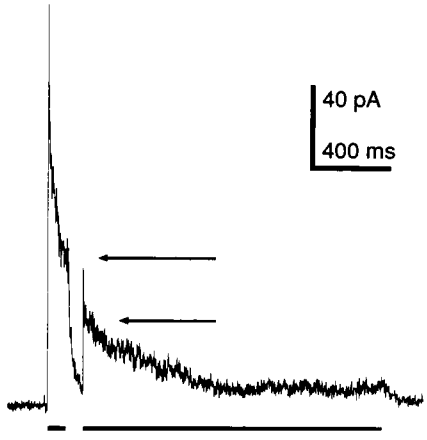

FIGURE 7 The fast and slow components are interconvertible. A brief application of 1 mM GABA (255 ms) was followed first by a brief wash period (180 ms), and then by a second application of 1 mM GABA. The first application completely desensitized the fast component. If the fast component is mediated by a separate population, the current at the beginning of the wash (indicated by the upper arrow) is mediated exclusively by receptors that desensitize slowly. During the wash period, little recovery from desensitization occurred as indicated by the of the magnitude of the peak response to the second application. The response to the second application desensitized with biphasic kinetics. The slow phase of the second application (lower arrow) was smaller than the current at the beginning of the wash period. All measurements are made relative to the baseline current before the first application. Holding potential: 0 mV, intracellular Cl^-: 46 mM. Similar results were obtained in seven other patches.

and Fischbach, 1989), this result does not exclude the possibility that the fast phase is mediated by a separate population of GABA$_A$ receptors with both high and low affinity sites, and that ligand binding to the high affinity site would lead to desensitization.

To examine this question further, we looked for evidence of interconversion among the different phases. In a series of eight patches, a brief application of 1 mM GABA (200–300 ms) was followed by a wash (150–250 ms) and then by a second 1 mM GABA application (Fig. 7). During the first application, the fast phase of desensitization was essentially complete, whereas the slower phases were only partially complete. The average current at the beginning of the wash period (upper arrow) was 34.6 ± 2.7% of the peak current. During the wash period, little or no recovery had occurred, and the peak response to the second application was 37.8 ± 4.4% of the peak response to the first application. About one-third of the response to the second application desensitized with rapid kinetics, and the magnitude of the slower phases (23.6 ± 2.8% of the peak response to the first application, lower arrow) was significantly less ($p < 0.005$, paired *t*-test) than the magnitude of the current at the beginning of the wash (upper arrow). These results are consistent with interconversion between the fast phase and the slower phases. The entire response is most likely mediated by a single population of receptors with multiple rates of desensitization. When a fraction of the population is desensitized, the remaining receptors are still capable of multiphasic desensitization.

Kinetic model of GABA$_A$ receptor activation and desensitization

We propose that the three phases of desensitization reflect equilibration between an activatable state and three desensitized states. The fast phase of desensitization is only observed when the rate of activation substantially exceeds the rate of desensitization. Because the rate of association is slow for relatively low GABA concentrations, equilibration between the activatable state and the fast desensitized state occurs before the maximum level of activation is attained. The fast phase of desensitization, therefore, is not observed. As the GABA concentration increases, the rate of activation increases (Fig. 8). When the activation rate is sufficiently fast relative to desensitization, activation precedes desensitization; the latter process will then occur subsequent to the peak response at fast, intermediate, and slow rates.

The model presented in Fig. 9 demonstrates the plausibility of this interpretation. The following assumptions are made: 1) the unbound receptor does not spontaneously desensitize; 2) binding of a single agonist is sufficient to activate the receptor; 3) gating is fast relative to binding and desensitization; and 4) all three desensitization reactions begin simultaneously with the binding of GABA. A single GABA binding step is used because the low Hill coefficients do not justify the requirement of additional GABA binding to open the channel. Models that require two GABA molecules to open the channel, however, are equally plausible when the rate constants are properly chosen.

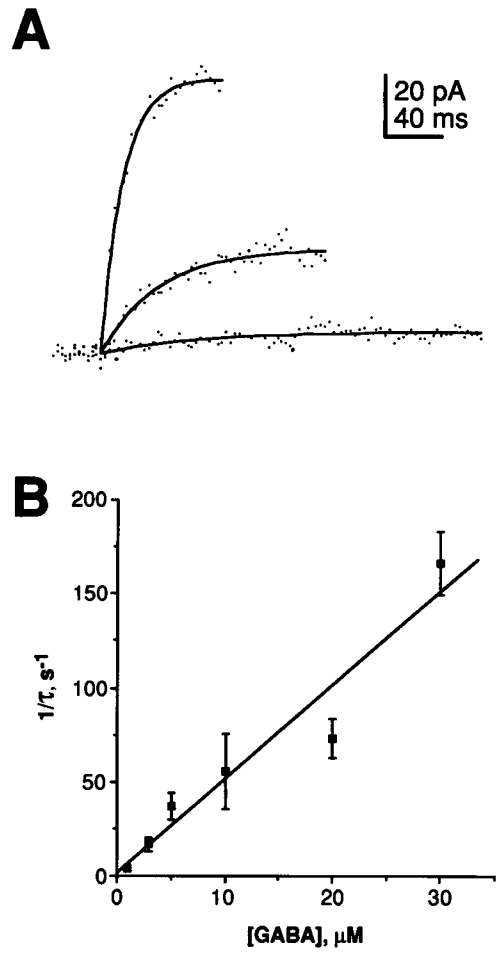

FIGURE 8 The rate of rise of the GABA response is linearly related to GABA concentration. (*A*) Initial responses to 3, 10, and 30 μM GABA recorded from the same patch. Data were fit to single exponentials (smooth curves). Holding potential: 0 mV, intracellular Cl^-: 46 mM. (*B*) Plot of the inverse of the rise time constants (as determined in *A*) against GABA concentration. Each point represents the average of $\geq$8 patches $\pm$ SE. The straight line was determined by linear regression and has a slope of 4.965 $\times$ 10^6 M^{-1} s^{-1}.

Rate constants were determined using experimental results. The equilibrium constants for the conversion of the activatable state (RA) to the fast (D_f) and intermediate (D_i) desensitized states were determined using the ratios of the relative maxima shown in Fig. 4. After equilibration between RA and D_f at saturating agonist, the fraction of receptors in RA is 0.757 (0.7839/1.036), giving an equilibrium constant of 3.11 (0.757/0.243). After equilibration with both D_f and D_i, the fraction of receptors in RA is 0.468 (0.4853/1.036), and after equilibration with all three desensitized states, a value of 0.053 (average I_{ss}/I_p for 1 mM GABA) is used for RA. The forward and reverse rate constants (k_f, and k_r) for the fast, intermediate, and slow reactions were derived using the equilibrium constants and the formula $1/\tau = (RA \times k_f) + k_r$, where τ is the desensitization time constant for 1 mM GABA (15.4, 207, and 1372 ms, respectively), and RA is the fraction of receptors in RA at the end of the previous phase of desensitization (1, 0.757, and 0.468, respectively).

To model the kinetics of GABA binding, we first measured the rate of activation by fitting the rising phase of the GABA response to a single exponential (Fig. 8). The reciprocal of the time constant was proportional to the GABA concentration with a slope of 4.97 $\times$ 10^6 M^{-1} s^{-1}. The forward rate constant for agonist binding used in this model (2.97 $\times$ 10^6 M^{-1} s^{-1}) was determined empirically and gives a slope of 4.74 $\times$ 10^6 M^{-1} s^{-1} when the inverse of the simulated rise time constant is plotted against agonist concentration (as in Fig. 8). During washout, the experimental GABA response decayed with a time constant of about 230 ms (see Figs. 6 and 7). This predicts a dissociation rate constant of 4.35 s^{-1} and a binding K_d of 1.47 μM. Because we were interested in modeling activation and desensitization, we calculated the dissociation rate constant (43.1 s^{-1}) based on a binding K_d equal to the observed EC_{50} of 14.5 μM.

Fig. 9 *A* shows a series of traces simulating the response to increasing GABA concentrations. Normally distributed random noise was added after simulation. Results were analyzed in a manner similar to the experimental data, and plots corresponding to Figs. 3 and 4 are shown in Fig. 9. Although there are subtle differences between experimental and simulated data, many features are common to both. The model shows a similar increase in the complexity of desensitization with increasing GABA. The effect of concentration on the extent of desensitization is greater than on the time constants of desensitization. Desensitization time constants for 1 mM GABA (17.9, 216, and 1577 ms) are similar to experimental values. The magnitudes of the three components of desensitization have well defined maxima and substantially different EC_{50} values, which are comparable to the experimentally observed values.

DISCUSSION

$GABA_A$ receptor desensitization

When the seven-barrel flow tube was used to apply high concentrations of GABA to outside-out patches, the desensitization was faster and more complex than any reported to date. The rate and magnitude of the fastest phase were both independent of the direction of current flow consistent with a true loss of channel mediated conductance rather than a loss of the Cl^- gradient. Open channel block by GABA at high concentrations is not likely because such a mechanism predicts both an increase in the desensitization rate without an increase in the peak response (Dilger and Liu, 1992), and a rebound response during washout (Maconochie and Knight, 1992). Neither of these effects was observed in this study.

In membrane vesicles, the two phases of desensitization did not interconvert (Cash and Subbarao, 1987), suggesting the presence of two separate receptor populations. In the present study, the different phases have similar ion selectivities and are capable of interconversion, consistent with a single population of receptors. The different findings could be because the vesicles are primarily pre- and postsynaptic membranes (Whittaker, 1969) prepared from the entire cerebral cortex, whereas patches used here were excised from

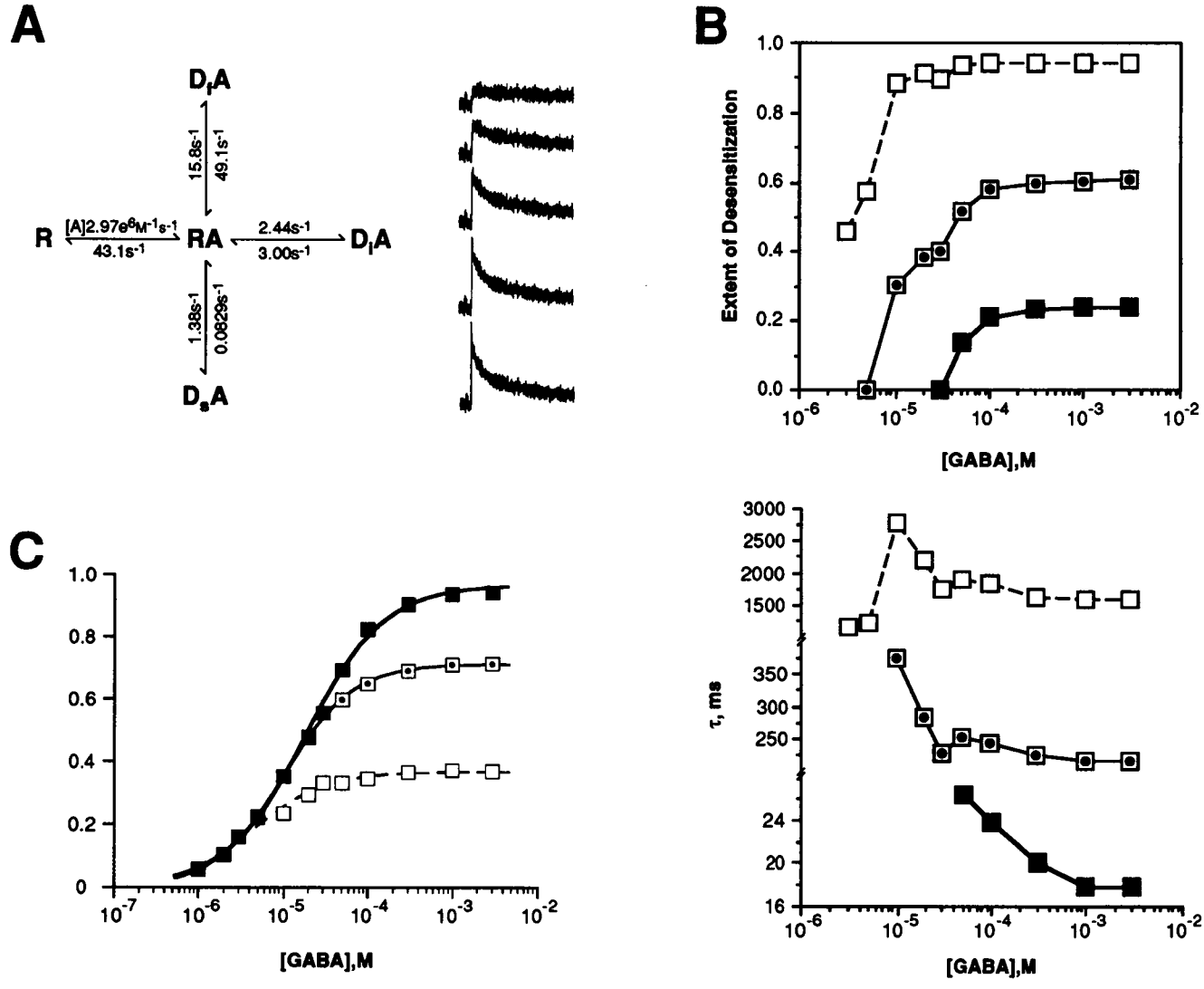

FIGURE 9 Kinetic model of GABA$_A$ receptor activation. (*A*) The unbound receptor (R) binds a single agonist and enters the activated form (RA). D_f, D_i, and D_s represent the states responsible for the fast, intermediate, and slow phases of desensitization, respectively. Simulated traces show the response to (from top) 3, 10, 30, 100, and 1000 μM GABA. Normally distributed noise was added to simulation results. (*B*) Desensitization of simulated results (with noise) was fit to one, two, or three component exponentials. The F-test was used to determine the number of components giving the best fit. Desensitization parameters were similar to those associated with experimental data (compare with Fig. 3). (*C*) GABA dose-response curve as in Fig. 4. Peak response had a maximum of 0.964, an EC_{50} of 19 μM, and a Hill coefficient of 0.93. The intermediate component has a maximum of 0.713, an EC_{50} of 10.2 μM, and a Hill coefficient of 1.06. The slow component has a maximum of 0.368, an EC_{50} of 4.33 μM, and a Hill coefficient of 1.00.

the cell bodies of a specific cell type. Changes in subunit composition can affect desensitization (Verdoorn et al., 1990), and given the large number of possible subunit combinations (Olsen and Tobin, 1990), region-specific heterogeneity is not unexpected (Houser et al., 1988; Shivers et al., 1989; Wisden et al., 1992).

The presence of three phases of desensitization made characterization of the effects of concentration on desensitization rates difficult. Although for a given concentration more than one pattern of desensitization was noted, three inherent time constants for the three phases were identified. The concentration-dependent increase in the overall rate of desensitization is attributed to the development of additional components of desensitization. Similar results were observed with glutamate receptor desensitization (Trussell and Fischbach, 1989). Desensitization of the response to 0.1 mM glutamate was best fit by a single exponential with an average time constant of 11.4 ms. Desensitization of the response to 1 mM glutamate had an average time constant of 4.8 ms when fit to a single exponential. In 11 out of 15 patches, however, desensitization was best fit by a double exponential with average time constants of 13.5 and 2.2 ms. As in the case of the GABA$_A$ receptor reported here, the apparent increase in desensitization rate of the glutamate receptor may be attributable to development of a faster phase without a significant change in the rate of the slower phase.

The three phases of $GABA_A$ receptor desensitization imply the existence of three separate desensitized states. Given the complex patterns of single channel kinetics (Macdonald et al., 1989; Weiss and Magleby, 1989; Twyman et al., 1990), it is not unreasonable to postulate the existence of multiple nonconducting states. It has been suggested for the acetylcholine receptor that the "fast" rate of desensitization (time constant of several seconds) corresponds to the average cluster length, and that the "ultra-fast" rate of desensitization (time constant of tens of milliseconds) corresponds to the average burst length (Cachelin and Colquhoun, 1989). It is interesting to note, for $GABA_A$ receptors in spinal cord neurons, that the longest of the three mean channel open times (11.3 ms, Macdonald et al., 1989) is comparable to the rate of rapid desensitization reported in this study (15.4 ms). The effect of increasing GABA in the single-channel study was to increase the relative magnitude of the component with the longest open time while not affecting the time constant. In the present study, the effect of increasing GABA was to increase the magnitude of the fast phase of desensitization without significantly affecting the inherent time constant. In the single channel study, the increase in GABA (from 0.5 to 5 μM) probably increased receptor occupancy, whereas in the present study the increase in GABA (above 30 μM) probably increased the rate of association. The increased rate of association has the effect of synchronizing receptor activation thereby revealing the fast phase of desensitization as a fraction of receptors close, following a single opening (mean open time of approximately 11 ms), and enter a desensitized state. Patches with fewer channels are less likely to have a large enough number of synchronized receptors to show a clearly discernible fast phase of desensitization. Preliminary simulation results utilizing a stochastic model of channel activity confirm that the signal-to-noise ratio for the fast phase of desensitization increases as the number of channels increases from 50 to 800.

Previous studies looking at the GABA dose-response curve report Hill coefficients close to 2 (Takeuchi and Takeuchi, 1967; Choi and Fischbach, 1981; Kaneda et al., 1989), whereas in the present study Hill coefficients were close to unity. We are unsure whether this difference is the result of the use of rapid application, or whether the $GABA_A$ receptors on CA1 pyramidal cells are truly different from those obtained from other sources. It is interesting to note that Hill coefficients are substantially affected by subunit composition, and that receptors in which $\alpha 1$ is the only α subunit consistently show Hill coefficients near unity (Sigel et al., 1990). Both antibody studies (Houser et al., 1988) and mRNA hybridization studies (MacLennan et al., 1991) suggest a preponderance of the $\alpha 1$ subunit in the CA1 region of the hippocampus. Although a low Hill coefficient suggests that a single GABA molecule is sufficient to open the channel, we cannot rule out the possibility that two molecules bind with low or slightly negative cooperativity, or that the channel is gated by two GABA binding sites with substantially different affinities.

Model of GABA receptor activation

We propose that multiphasic desensitization is explained simply by the existence of three desensitized states and the increased rate of association at higher concentrations. The kinetic model is presented solely to demonstrate the plausibility of this, and to show that additional GABA binding sites or multiple receptor populations need not be postulated to explain multiphasic desensitization.

We make the assumption that gating is fast relative to binding. Although the association reaction of the acetylcholine receptor is believed to be diffusion-limited (10^8 M^{-1} s^{-1}, Colquhoun and Sakmann, 1985), slower rates have been reported for the glutamate (Kerry et al., 1988; Clements and Westbrook, 1991) and $GABA_A$ (Twyman et al., 1990) receptors. In this study, the activation time for 1 mM GABA was typically no more than 1 ms. This corresponds to gating kinetic constants on the order of 1000 s^{-1}, which are comparable to those seen in cerebral neurons (Weiss and Magleby, 1989), but faster than those seen in spinal cord neurons (Macdonald et al., 1989). A model in which binding was rapid relative to gating would require an extremely fast dissociation rate constant (>1000 s^{-1}), which contradicts the slow washout of the GABA response seen in this study (see Fig. 6 for example). By simulating the response to various concentrations of GABA, our model reproduces the general features of the experimental results.

Future studies

We developed the seven-barrel flow tube with the intention of combining the flexibility of the seven-barrel puffer system (Chan et al., 1983; Chan and Farb, 1985; Celentano et al., 1991) and the speed of the more recently developed flow tube systems (Brett et al., 1986; Franke et al., 1987; Maconochie and Knight, 1989). This will be ideal for studying the dose-response curves of lipophilic drugs that cannot be reliably washed out of drug delivery systems during the course of an experiment.

Our initial motivation for beginning this study was to explore the effects of $GABA_A$ receptor modulators on the complete GABA dose-response curve. The whole-cell configuration proved inappropriate for the study of the fast phase of desensitization because of the fast kinetics. Rise times in whole CA1 pyramidal neurons were slow despite high concentrations of GABA, and the fast phase of desensitization was not observed. At this time, we cannot rule out the possibility that the rapid phase of desensitization is unique to outside-out patches. Differences in $GABA_A$ receptor desensitization kinetics between outside-out patches and intact membranes have been reported in cultured hippocampal neurons (Frosch et al., 1992).

Whole-cell studies were also limited by the dramatically high conductances induced by high concentrations of GABA. We estimate that in the presence of 1 mM GABA, the input resistance of whole cells drops to 7.4 MΩ, which is comparable to the electrode resistance making an accurate voltage clamp nearly impossible. The high density of

GABA$_A$ receptors on these cells is probably due to the high density of GABAergic synaptic contacts made on the cell bodies of hippocampal pyramidal neurons in vivo (Ribak et al., 1978; Somogyi et al., 1983). As a result of this high density, outside-out patches contained a sufficient number of receptors to enable us to study the macroscopic effects of rapid application of GABA. Relatively few receptors are found on patches excised from cultured neurons (Macdonald et al., 1989; Weiss and Magleby, 1989), which may not have the same density of synaptic contacts.

With the present approach, details of the GABA$_A$ response are described for the first time. It would be of interest to reevaluate the effects of modulators on the GABA$_A$ receptor response by studying the effects of modulators on the response to rapidly applied GABA in outside-out patches. Preliminary results are consistent with an increase in affinity induced by phenobarbital and 5β-pregnan-3α-*ol*-20-one (Celentano and Wong, 1993). In addition, because the GABA$_A$ response in these cells is controlled by intracellular agents, possibly via phosphorylation processes, a detailed understanding of this control process should include a study on the effects of intracellular modulators on the multiphasic desensitization of the GABA$_A$ response.

We thank Drs. Terrell T. Gibbs and David H. Farb for helpful discussion. Supported by grants T32 NS 07117 and NS 24682 from the National Institutes of Health.

REFERENCES

Akaike, N., M. Inoue, and O. A. Krishtal. 1986. "Concentration-clamp" study of γ-aminobutyric-acid-induced chloride current kinetics in frog sensory neurones. *J. Physiol. (Lond.)*. 379:171–185.

Ben-Ari, Y., K. Krnjevic, and W. Reinhardt. 1979. Hippocampal seizures and failure of inhibition. *Can. J. Physiol. Pharmacol.* 57:1462–1466.

Brett, R. S., J. P. Dilger, P. R. Adams, and B. Lancaster. 1986. A method for the rapid exchange of solutions bathing excised membrane patches. *Biophys. J.* 50:987–992.

Cachelin, A. B., and D. Colquhoun. 1989. Desensitization of the acetylcholine receptor of frog end-plates measured in a vaseline-gap voltage clamp. *J. Physiol. (Lond.)* 415:159–188.

Cash, D. J., and K. Subbarao. 1987. Desensitization of γ-aminobutyric acid receptor from rat brain: two distinguishable receptors on the same membrane. *Biochemistry*. 26:7556–7562.

Celentano, J. J., T. T. Gibbs, and D. H. Farb. 1991. Negative modulation of the γ-aminobutyric acid response by extracellular zinc. *Mol. Pharmacol.* 40: 766–773.

Celentano, J. J., and R. K. S. Wong. 1993. Effects of phenobarbital and 5β-pregnan-3α-ol-20-one on the GABA$_A$ receptor from CA1 pyramidal cells. *Neurosci. Abstr.* 19:1538a. (Abstr.)

Chan, C. Y., and D. H. Farb. 1985. Modulation of neurotransmitter action: control of the γ-aminobutyric acid response through the benzodiazepine receptor. *J. Neurosci.* 5:2365–2373.

Chan, C. Y., T. T. Gibbs, L. A. Borden, and D. H. Farb. 1983. Multiple embryonic benzodiazepine binding sites: evidence for functionality. *Life Sci.* 33:2061–2069.

Chen, Q. X., A. Stelzer, A. R. Kay, and R. K. S. Wong. 1990. GABA$_A$ receptor function is regulated by phosphorylation in acutely dissociated guinea-pig hippocampal neurons. *J. Physiol. (Lond.)*. 420:207–221.

Choi, D. W., and G. D. Fischbach. 1981. GABA conductance of chick spinal cord and dorsal root ganglion neurons in cell culture. *J. Neurophysiol.* 45:605–620.

Clements, J. D., and G. L. Westbrook. 1991. Activation kinetics reveal the number of glutamate and glycine binding sites on the N-methyl-D-aspartate receptor. *Neuron*. 7:605–613.

Colquhoun, D. 1971. Lectures on Biostatistics. Clarendon Press, Oxford, UK. 425 pp.

Colquhoun, D., and B. Sakmann. 1985. Fast events in single-channel currents activated by acetylcholine and its analogues at the frog muscle end-plate. *J. Physiol. (Lond.)*. 369:501–557.

De Lean, A. P., P. J. Munson, and D. Rodbard. 1978. Simultaneous analysis of families of sigmoidal curves: application to bioassay, radioligand assay, and physiological dose-response curves. *Am. J. Physiol.* 235: E97–E102.

Dilger, J. P., and Y. Liu. 1992. Desensitization of acetylcholine receptors in BC3H-1 cells. *Pflügers Arch.* 420:479–485.

Dudel, J., C. Franke, and H. Hatt. 1992. Rapid activation and desensitization of transmitter-liganded receptor channels by pulses of agonists. *In* Ion Channels. T. Narahashi, editor. Plenum Press, New York. 207–260.

Franke, C., H. Hatt, and J. Dudel. 1987. Liquid filament switch for ultra-fast exchanges of solutions at excised patches of synaptic membrane of crayfish muscle. *Neurosci. Lett.* 77:199–204.

Franke, C., H. Hatt, H. Parnas, and J. Dudel. 1991. Kinetic constants of the aceylcholine (ACh) receptor reaction deduced from the rise in open probability after steps in ACh concentration. *Biophys. J.* 60:1008–1016.

Frosch, M. P., S. A. Lipton, and M. A. Dichter. 1992. Desensitization of GABA-activated currents and channels in cultured cortical neurons. *J. Neurosci.* 12:3042–3053.

Gray, R., and D. Johnston. 1985. Rectification of single GABA-gated chloride channels in adult hippocampal neurons. *J. Neurophysiol.* 54: 134–142.

Gyenes, M., M. Farrant, and D. H. Farb. 1988. "Run-down" of γ-aminobutyric acid$_A$ receptor function during whole-cell recording: a possible role for phosphorylation. *Mol. Pharmacol.* 34:719–723.

Haefely, W., and P. Polc. 1986. Physiology of GABA enhancement by benzodiazepines and barbiturates. *In* Benzodiazepine/GABA Receptors and Chloride Channels: Structural and Functional Properties. R. W. Olsen and C. J. Venter, editors. Alan R. Liss, Inc., New York. 97–133.

Hamill, O. P., A. Marty, E. Neher, B. Sakmann, and F. J. Sigworth. 1981. Improved patch-clamp techniques for high-resolution current recording from cells and cell-free membrane patches. *Pflügers Arch.* 391:85–100.

Holland, K. D., K. W. Yoon, J. A. Fererndelli, D. F. Covey, and S. M. Rothman. 1990. γ-Butyrolactone antagonism of the picrotoxin receptor: comparison of a pure antagonist and a mixed antagonist/inverse agonist. *Mol. Pharmacol.* 39:79–84.

Hooke, R., and T. A. Jeeves. 1961. "Direct search" solution of numerical and statistical problems. *J. Ass. Comput. Mach.* 8:212–229.

Houser, C. R., R. W. Olsen, J. G. Richards, and H. Möhler. 1988. Immunohistochemical localization of benzodiazepine/GABA$_A$ receptors in the human hippocampal formation. *J. Neurosci.* 8:1370–1383.

Kaneda, M., M. Wakamori, and N. Akaike. 1989. GABA-induced chloride current in rat isolated Purkinje cells. *Am. J. Physiol.* 256:C1153–C1159.

Kay, A. R., and R. K. S. Wong. 1986. Isolation of neurons suitable for patch-clamping from adult mammalian central nervous systems. *J. Neurosci. Methods.* 16:227–238.

Kerry, C. J., R. L. Ramsey, M. S. P. Sansom, and P. N. R. Usherwood. 1988. Glutamate receptor channel kinetics: the effect of glutamate concentration. *Biophys. J.* 53:39–52.

Kirkness, E. F., and A. J. Turner. 1988. The stimulatory effects of secobarbital and pregnanolone on the GABA$_A$ receptor can be blocked selectively. *Eur. J. Pharmacol.* 150:385–388.

Kreider, J. F. 1985. Principles of Fluid Mechanics. Allyn and Bacon, Inc., Boston. 609 pp.

Krnjevic, K. 1974. Chemical nature of synaptic transmission in vertebrates. *Physiol. Rev.* 54:418–540.

Macdonald, R. L., C. J. Rogers, and R. Twyman. 1989. Kinetic properties of the GABA$_A$ receptor main conductance state of mouse spinal cord neurones in culture. *J. Physiol. (Lond.)*. 410:479–499.

MacLennan, A. J., N. Brecha, M. Khrestchatisky, C. Sternini, N. J. K. Tillakaratne, M.-Y. Chiang, K. Anderson, M. Lai, and A. J. Tobin. 1991. Independent cellular and ontogenetic expression of mRNAs encoding three α polypeptides of the rat GABA$_A$ receptor. *Neurosci.* 43:369–380.

Maconochie, D. J., and D. E. Knight. 1989. A method for making solution changes in the sub-millisecond range at the tip of a patch pipette. *Pflügers Arch.* 414:589–596.

Maconochie, D. J., and D. E. Knight. 1992. A study of the bovine adrenal chromaffin nicotinic receptor using patch clamp and concentration-jump techniques. *J. Physiol. (Lond.).* 454:129–153.

Mierlak, D., and D. H. Farb. 1988. Modulation of neurotransmitter receptor desensitization: chlordiazepoxide stimulates fading of the GABA response. *J. Neurosci.* 8:814–820.

Motulsky, H. J., and L. A. Ransnas. 1987. Fitting curves to data using nonlinear regression: a practical and nonmathematical review. *FASEB J.* 1:365–374.

Munson, P. J., and D. Rodbard. 1980. LIGAND: a versatile computerized approach for characterization of ligand-binding systems. *Anal. Biochem.* 107:220–239.

Nedler, J. A., and R. Mead. 1965. A simplex method for function minimization. *Comp. J.* 7:308–313.

Newland, C. F., D. Colquhoun, and S. G. Cull-Candy. 1991. Single channels activated by high concentrations of GABA in superior cervical ganglion neurones of the rat. *J. Physiol. (Lond.).* 432:203–233.

Numann, R. E., and R. K. S. Wong. 1984. Voltage-clamp study on GABA response desensitization in single pyramidal cells dissociated from the hippocampus of adult guinea pigs. *Neurosci. Lett.* 47:289–294.

Oh, D. J., and M. A. Dichter. 1992. Desensitization of GABA-induced currents in cultured rat hippocampal neurons. *Neuroscience.* 49:571–576.

Olsen, R. W. 1982. Drug interactions at the GABA receptor-ionophore complex. *Ann. Rev. Pharmacol. Toxicol.* 22:245–277.

Olsen, R. W., and A. J. Tobin. 1990. Molecular biology of $GABA_A$ receptors. *FASEB J.* 4:1469–1480.

Ribak, C. E., J. E. Vaughn, and K. Saito. 1978. Immunocytochemical localization of glutamic acid decarboxylase in neuronal somata following colchicine inhibition of axonal transport. *Brain Res.* 140:315–332.

Sather, W., J. W. Johnson, G. Henderson, and P. Ascher. 1990. Glycine-insensitive desensitization of NMDA responses in cultured mouse embryonic neurons. *Neuron.* 4:725–731.

Shivers, B. D., I. Killisch, R. Sprengel, H. Sontheimer, M. Köhler, P. R. Schofield, and P. H. Seeburg. 1989. Two novel $GABA_A$ receptor subunits exist in distinct neuronal subpopulations. *Neuron.* 3:327–337.

Sigel, E., R. Baur, G. Trube, H. Möhler, and P. Malherbe. 1990. The effect of subunit composition of rat brain $GABA_A$ receptors on channel function. *Neuron.* 5:703–711.

Sivilotti, L., and A. Nistri. 1991. GABA receptor mechanisms in the central nervous system. *Prog. Neurobiol.* 36:35–92.

Somogyi, P., A. D. Smith, M. G. Nunzi, A. Gorio, H. Takagi, and J. Y. Wu. 1983. Glutamate decarboxylase immunoreactivity in the hippocampus of the cat: distribution of immunoreactive synaptic terminals with special reference to the axon initial segment of pyramidal neurons. *J. Neurosci.* 3:1450–1468.

Stelzer, A., A. R. Kay, and R. K. S. Wong. 1988. $GABA_A$-receptor function in hippocampal cells is maintained by phosphorylation factors. *Science.* 241:339–341.

Takeuchi, A., and N. Takeuchi. 1967. Anion permeability of the inhibitory post-synaptic membrane of the crayfish neuromuscular junction. *J. Physiol. (Lond.).* 191:575–590.

Thalmann, R. H., and N. Hershkowitz. 1985. Some factors that influence the decrement in the response to GABA during its continuous iontophoretic application to hippocampal neurons. *Brain Res.* 342:219–233.

Trifiletti, R. R., A. M. Snowman, and S. H. Snyder. 1985. Barbiturate recognition site on the GABA/benzodiazepine receptor complex is distinct from the picrotoxinin/TBPS site. *Eur. J. Pharmacol.* 106:441–447.

Trussell, L. O., and G. D. Fischbach. 1989. Glutamate receptor desensitization and its role in synaptic transmission. *Neuron.* 3:209–218.

Twyman, R. E., C. J. Rogers, and R. L. Macdonald. 1990. Intraburst kinetic properties of the $GABA_A$ receptor main conductance state of mouse spinal cord neurones in culture. *J. Physiol. (Lond.).* 423:193–220.

Verdoorn, T. A., A. Draguhn, S. Ymer, P. H. Seeburg, and B. Sakmann. 1990. Functional properties of recombinant rat $GABA_A$ receptors depend upon subunit composition. *Neuron.* 4:919–928.

Weiss, D. S., and K. L. Magleby. 1989. Gating scheme for single GABA-activated Cl^- channels determined from stability plots, dwell-time distributions, and adjacent-interval durations. *J. Neurosci.* 9:1314–1324.

Whittaker, V. P. 1969. The synaptosome. *In* Handbook of Neurochemistry. A. Lajtha, editor. Plenum Press, New York. 327–364.

Wisden, W., D. J. Laurie, H. Monyer, and P. H. Seeburg. 1992. The distribution of 13 $GABA_A$ receptor subunit mRNAs in the rat brain. I. Telencephalon, diencephalon, mesencephalon. *J. Neurosci.* 12:1040–1062.

Zar, J. H. 1984. Biostatistical Analysis. Prentice-Hall, Inc., Englewood Cliffs, NJ. 736 pp.